

## Energy Engineering

# Electrical Characteristics of SnS /ZnS Heterojunction

M. Messaoudi<sup>1, 2 a \*</sup>, L. Beddek<sup>3, b</sup>, M. Maiza<sup>1, c</sup> M.S. Aida<sup>4, d</sup>, N. Attaf<sup>2, e</sup> and H. Nezzari<sup>1, f</sup>

<sup>1</sup>Research Center in Industrial Technologies CRTI, P. O. Box 64, Cheraga 16014, Algiers, Algeria

<sup>2</sup>Thin Films and Interfaces Laboratory, University of Frères Mentouri Constantine, 25000 Constantine, Algeria

<sup>3</sup>Department of physics, University of moloud Mammeri Tizi-Ouzou, Algeria

<sup>4</sup>Department of physics, King Abdulaziz University, Jeddah, Makkah Province, Saudi Arabia

<sup>a\*</sup> messaoudi\_phlmd@yahoo.fr

<sup>b</sup> beddeklynda@hotmail.fr

<sup>c</sup> mounira1990@live.com

<sup>d</sup> aida\_salah2@yahoo.fr

<sup>e</sup> nattaf1@yahoo.fr

<sup>f</sup> h.nezzari@crti.dz / \* nezzari.h@gmail.com

**Abstract.** Thin sulphide (SnS) is a promising candidate for a low cost, no toxic solar cells absorber layer. In this paper thin films of SnS were prepared by spray pyrolysis onto glass and ZnS/FTO coated glass substrates at different substrate temperatures in the range 250–400°C. SnS were characterized with X-rays diffraction and scanning electron microscopy and UV visible transmittance. The electrical properties of SnS/ZnS heterojunctions were determined using recording their current-voltage I(V) and capacitance-voltage (C-V) characteristics at ambient and at different measurement temperatures from 28–94°C. The results analysis indicate that the saturation current varied from 0.68 to 2.8  $\mu$ A and series resistance from 191 to 800  $\Omega$ . The structures ideality factor is ranged from 1.37 to 2.7. The diffusion potential ( $V_d$ ) was determined by the intercept of extrapolation of  $1/C^2$ -V curve to the abscise axis ( $V=0$ ) we found  $V_d$  values ranged from 0.67 to 1.2 V.

**Keywords:** Tin sulfide; thin films; solar cell; spray pyrolysis; SnS/CdS Heterojunction.

## INTRODUCTION

In these last years, more than 90% of the solar cells are based in semiconductor thin films, like CdTe, Cu(I, G)Se, CZTS and SnS absorbing layers. Cu(In,Ga)(S,Se)<sub>2</sub> is one of the most promising thin- film solar cell materials, demonstrating an efficiency of about 20%. However, In and Ga are expensive components, and the band gap is usually not optimal for high efficiency CIGS solar cells. Currently, designing and synthesizing novel, high-efficiency, and low cost solar cell absorbers to replace CIGS has attracted much attention. Among the materials that have been investigated, binary system tin (II) sulfide. SnS is one of the most abundant elements on the earth perfectly stable, no toxic and a p-type semiconductor with a direct band gap 1.3eV [1, 2]. The percentage of constituents the SnS phase can be accompanied with other complexes consisting mainly of SnS<sub>2</sub>, Sn<sub>2</sub>S<sub>3</sub> and Sn<sub>3</sub>S<sub>4</sub>; depending on system and temperature of preparation. The SnS and SnS<sub>2</sub> compounds are the most stable [3].

The solar cell, having the structure Mo/p- SnS/n-CdS/ZnO heterojunctions have an open circuit voltage of 260 mV, a short circuit current density of 9.6 mA/cm<sup>2</sup>, a fill factor of 0.5 and energy efficiency of 1.3% in 2006 formed by Reddy, et al [4]. The SnS layer in this device was synthesized by spray pyrolysis method. In 2008, Ghosh et al [5]. Solar cells have also been made using the SnS layers, usually using CdS as the n- type partner layer and efficiencies up to 2% have been observed in the best devices. A combination of Voc of 244 mV, and h of 2.04% for

active cell area of 0.71 cm<sup>2</sup> has been reported in 2013 for a solar cell structure, glass/Mo/SnS/Zn(O,S)/ZnO/ITO, was deposited via pulsed-CVD to one fabricated by Sinsermsuksakul et al. [6].

SnS thin film mostly crystallize in the orthorhombic (OR) structure, when formed via spray pyrolysis [7], chemical deposition [8], electrochemical [9], thermal evaporation [10], atomic layer deposition (ALD) [11].

In this work, we have showed the effect of substrate temperature on electrical properties of SnS /ZnS heterojunction deposited by spray pyrolysis technique. Series resistance, ideality factor, current saturation and diffusion potential were determined by I-V and C-V characteristics.

## EXPERIMENTAL

In this study, the studied structure is Au/p- SnS/n-ZnS/FTO heterojunctions deposited on a glass substrate, these layers prepared by the same spray pyrolysis technique. The first thin films is FTO (tin oxide doped by Fluor which belong transparent oxide conductor TCO); were prepared at substrates temperature of 450°C. The substrate carefully cleaned in acetone, ethanol and distilled water in sequence. For each step, the substrates were cleaned for 15 min in an ultrasonic bath. After a rinse with distilled water. FTO film was prepared using (0.1 M) SnCl<sub>2</sub>.2H<sub>2</sub>O as source of Tin and NH<sub>4</sub>F (10%) as source of Fluor. Second thin films is ZnS window layers were deposited onto the FTO films at substrates temperature of 400°C. The starting solution was a mixture of (0.1M) Zn(C<sub>2</sub>H<sub>3</sub>O<sub>2</sub>)<sub>2</sub>.2H<sub>2</sub>O as source of zinc and (0.05M) thiourea as source of sulphur.

The thickness of the FTO and ZnS films were about 200 nm, 120 nm. SnS thin layers have been grown, onto window layers at different substrate temperatures ranged from 300 to 400°C. The used solution is a mixture of SnCl<sub>2</sub>.2H<sub>2</sub>O and thiourea precursors dissolved in distilled water, the solution flow rate was maintained at 10 ml/h. The measured thicknesses values are varied in the range of 200-400 nm with increasing substrate temperature.

Finally, golden contacts are deposited onto absorber layer SnS by DC sputtering system. The I-V characteristic of the obtained hetero-structure was recorded using a curve tracer 370 Sony Tetronix.

## RESULTS AND DISCUSSION

### STRUCTURAL PROPERTIES

In figure 1 we have reported a typical XRD spectrum of SnS films prepared by spray pyrolysis technique with various substrate temperatures in the range 250 to 400°C. As can be seen, films grown at temperatures Ts = 250, 350 and 400°C, presence strong peak at 31.8 assigned to the plane (111) orientation of the SnS monophase orthorhombic structure. As can be seen, (111) plane is a preferential orientation. This is in consistent with the results of Reddy et al and T.H. Sajeesh et al [4, 12]. However, films deposited at Ts = 300°C show the presence of SnS and Sn<sub>2</sub>S<sub>3</sub> phases corresponding to the (112) and (150) planes respectively. Bellow 300 °C of substrate temperature, it has not been reported the presence of Sn<sub>2</sub>S<sub>3</sub> phase in films prepared by spray pyrolysis [12-14].

### SURFACE MORPHOLOGY

In figure 2 (b, c) we have reported the SEM images of SnS films prepared at 250 and 400°C substrate temperatures. As can be seen, films surface morphologies are dense and continuous. But films prepared at substrate temperature 250°C, small pores and pinholes are visible in films surfaces.

### OPTICAL PROPERTIES

The transmittance spectra of SnS films are display in fig.3. The optical transmittance versus wavelength in the visible range of different films is reported in figure 3(d). Films prepared at high substrate temperature have a larger transmittance then films deposited at low substrate temperature due to thickness films. Optical band gap Eg and absorption coefficient is related as:

$$(\alpha h\nu)^{1/p} = A(h\nu - E_g) \quad (1)$$

Where A is a constant, exponent p is the transition probability. For p = 1/2 the transition is direct and allowed, p=2 indirect and allowed and p =3/2 for direct forbidden.

To determine direct allowed band gap a graph between  $(h\nu)^2$  and  $h\nu$  is plotted and the straight portion of the graph is extrapolated to energy axis to give  $E_g$ . From figure 3(e) the band gap decreases from 1.11, 1.3 and 1.51eV with increase substrate temperature  $T_s = 250, 350$  and  $400^\circ\text{C}$  respectively. However, films grown at temperatures  $300^\circ\text{C}$  the energy gap 1.57eV. This is due to attributed to the presence of other phases of SnS such  $\text{Sn}_2\text{S}_3$ .

## I-V CHARACTERISTIC

Fig. 4 shows the current–voltage characteristic of the ZnS/SnS heterojunction with films of SnS prepared at  $350^\circ\text{C}$ ; Based on the dark current as a function of the applied bias,. This heterojunction measured at room temperature and at different temperatures from 28 to  $94^\circ\text{C}$  in the dark.

Curve  $I(V)$  to divide has two region, the first with low direct polarization if  $V$  vary between 0 and 1.5 and current varied exponentially with the tension, the current of the structure will be given by:

$$I = I_s (e^{(qV/nKT)})^{-1} \quad (2)$$

And is given below:

$$I_s = A^*T^2 \exp(-q\Phi_b / kBT) \quad (3)$$

Where  $q$  is the electronic charge,  $V$  is the applied voltage,  $k$  is the Boltzmann constant,  $n$  is the ideality factor,  $T$  is the temperature,  $\Phi_b$  is effective barrier height,  $A^*$  is effective Richardson constant and  $I_s$  is the reverse saturation current [15].

The second region with high direct polarization,  $V$  superior with 1.5V the current varies linearly with the tension it is written by:

$$I(v) = (1/R_s)V \quad (4)$$

The  $I-V$  curves of the devices show good rectifying behavior in a wide temperature range and the leakage current was very small at  $94^\circ\text{C}$ . The corresponding diode series resistance, defined as  $R_s = (dI/dV)^{-1}$ [16], which is obtained from the slope of high voltage region of  $I-V$  plots is decreases with the increase in measurement temperature.

The plot of  $\log I$  against  $V$  is shown in Fig.5(h). Which indicates that the current at low voltage ( $V < 1.2\text{V}$ ) varies exponentially with voltage. The characteristics can be described by the standard diode equation (2).

The value of the ideality factor of SnS/ZnS heterojunction is determined from the slope of the straight line region of the forward bias  $\log I-V$  characteristics and the saturation current  $I_s$  was obtained by extrapolating the forward characteristics  $\log I-V$  to zero voltage.

It can be seen, at the lower forward bias ( $V < 1.2\text{V}$ ), the values of the ideality factor and the reverse saturation current are 1.8 and  $1.04 \times 10^{-6}\text{A}$ , respectively, using the standard diode equation (2). From the result the ideality factor is varied between 1.37 and 2.7.

Where  $n=1.89$ ; this is close to 2 and  $I_s=1.04 \times 10^{-6}\text{A}$ . The result of the calculation (using the standard diode equation (2)) is similar to the measurement from the  $I-V$  curve. This result indicates that the recombination current ( $I_r = \exp(qV/2kT)$ ) dominates in this range.

At higher voltages ( $V > 1.2\text{V}$ ) the curves deviate from the exponential behavior, which is seen from the flattening of the characteristic curve. Indicating the effect of a series resistance. A simple series resistance model eq (4) can be applied in an attempt to linearism the characteristics. The series resistance of the ZnS/SnS heterojunction grows at  $350^\circ\text{C}$  substrate temperature from 394 to  $981 \Omega$ .

Fig.4(g) shows the Variation of the saturation current as a function of  $1000/T$ ; of the SnS films grow at different substrate temperature. The activation energy  $E_a$  is extracted from this plot is varied from 0.072 to 0.63 eV.

The barrier height,  $q\Phi_b$  is obtained from the saturation current variation with the temperature according to the relation (3). The value of potential barrier is varied between 0.78 and 0.25eV. It can be seen, the values of the potential barrier decreases with the increase in substrate temperature.

In the assumption of an abrupt junction, the reverse capacitance of a p-n junction can be expressed as [17]

$$1/C^2 = (V_b + V) \quad (5)$$

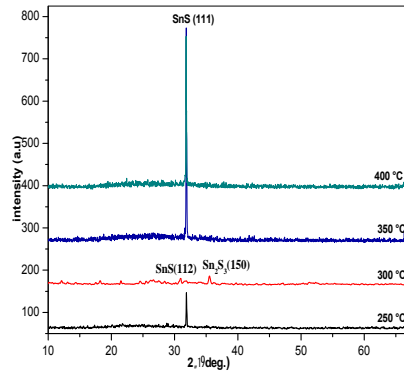
Where  $C$  is the reverse-bias capacitance and  $V$  is the reverse-bias voltage. A plot of  $(1/C^2 - V)$  intercept on the x-axis is essentially equal to the diffusion potential  $V_b$ . Fig.5(i) shows the C-V characteristics were measured. The capacitance values obtained yield a linear  $1/C^2$  versus  $V$  dependence with an intercept  $V_d$  values ranged from 0.67 to 1.2 V. The slope of the straight line gives donor concentration; (present in tableau 1).

## Tables

**TABLE 1.** Variation of the saturation current, ideality factor and potential barrier as a function of different substrates temperatures

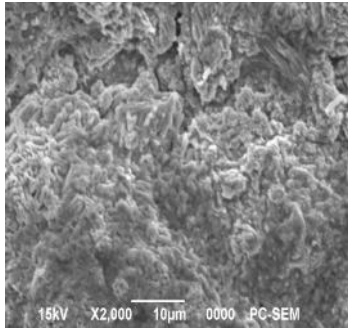
substrat température (°C)	Ideality factor	reverse saturation current(A)	QB(e V)	Vd (V)	Nd(m <sup>-3</sup> )
250	1.75	1.34X10 <sup>-6</sup>	0.46		8.07x10 <sup>23</sup>
300	1.76	0.6 X10 <sup>-6</sup>	0.21		2.11x10 <sup>23</sup>
350	1.8	1.02X10 <sup>-6</sup>	0.63		1.03x10 <sup>22</sup>
400	1.4	1.36 X10 <sup>-6</sup>	0.072		1.61x10 <sup>23</sup>

## Figures

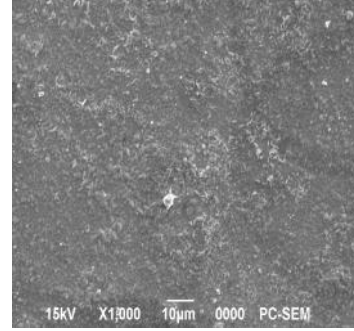


(a)

**FIGURE 1.** (a) : XRD patterns of tin sulfide film grown at 250 and 400°C substrate temperature.

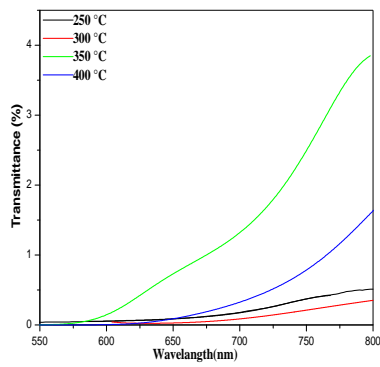


(b)

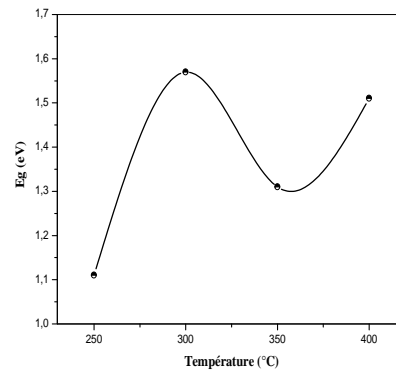


(c)

**FIGURE 2.** SEM image of SnS films deposited at different substrate temperature (b) 250°C and (c) 400°C.



(d)



(e)

**FIGURE 3.** (d) : UV-Visible transmittance spectrum of SnS thin films deposited at different substrate temperature.

(e) : Dependence of optical band gap on the deposition substrate temperature.

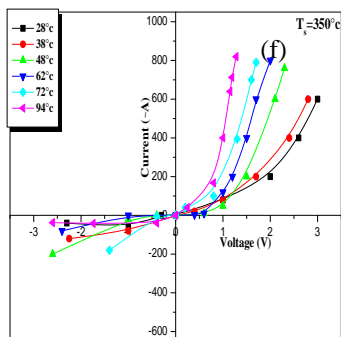
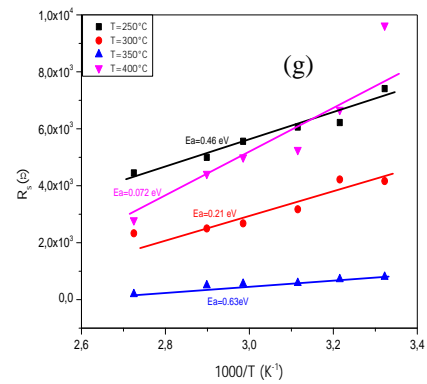


**FIGURE 4.** (f) : I-V curve of the SnS/ZnS heterojunction device in dark with SnS prepared at 350°C.



(g) : Variation of the series resistance as a function of temperature measurement.



**FIGURE 5.** (h) : The corresponding logarithmic scale in current with forward bias condition of ZnS/SnS heterojunction at room temperature of SnS film grow at 350°C.

(i) : The  $1/C^2$  -V of the ZnS/SnS heterojunction at substrate temperature:  $T_s = 350^\circ\text{C}$

## CONCLUSIONS

Heterojunction of ZnS/SnS has been fabricated with SnS thin films grown at different substrate temperature in the range 250-400°C; ZnS and SnS thin films are prepared by same technique spray ultrasonic. SnS single phase with orthorhombic structure and band gap equal 1.3eV are observed from the film as grown at 350°C. The results of characteristic I-V indicate that the saturation current varied from 0.68 to 2.8  $\mu\text{A}$  and series resistance from 191 to 800  $\Omega$ , The structures ideality factor is ranged from 1.37 to 2.7. The diffusion potential  $V_d$  values ranged from 0.67 to 1.2 V.

## REFERENCES

1. B. Ghosh, M. Das, P. Banerjee, S. Das, Fabrication and optical properties of SnS thin films by SILAR method, *Appl. Surf. Sci.* 254, 6436–6440, (2008).
2. A.R. Ettema, R.A. De Groot, C. Haas, T.S. Turner, Electronic structure of SnS deduced from photoelectron spectra and band-structure calculations, *Phys. Rev. B* 46 (12) 7363–7373, (1992).
3. A.C. Rastogi, K.S. Balakrishnan, G. Archanc, A new electrochemical selenization techniques for preparation of metal selenide semiconductor thin films, *Electrochem. Soc. Inc.* 140 (8) 2373–2375, (1993).
4. K.T.R. Reddy, N.K. Reddy, R.W. Miles, *Sol. Energy Mater. Sol. Cells* 90 3041, (2006).
5. Ghosh B, Das M, Banerjee P, Das S. Fabrication of vacuum evaporated SnS/CdS heterojunction for PV applications. *Sol. Energy Mat. Sol. Cells*; 92, 1099-1104, (2008).
6. P. Sinsermsuksakul, K. Hartman, S.B. Kim, J. Heo, L. Sun, H.H. Park, R. Chakraborty, T. Buonassisi, R.G. Gordon, *Appl. Phys. Lett.* 102 053901-1e053901-5, (2013).
7. M. Calixto-Rodriguez, H. Martinez, A. Sanchez-Juarez, J. Campos-Alvarez, A. Tiburcio-Silver, M.E. Calixto, *Thin Solid Films*, 517, 2497-2499, (2009).
8. C. Gao, H.L. Shen, *Thin Solid Films*, 520, 3523-3527, (2012).
9. J.R.S. Brownson, C. Georges, G. Larramona, A. Jacob, B. Delatouche, C. Levy-Clement, *J. Electrochem. Soc.*, 155, D40-D46, (2008).
10. S.S. Hegde, A.G. Kunjomana, M. Prashantha, C. Kumar, K. Ramesh, *Thin Solid Films*, 11. 545, 543-547, (2013).
12. J.Y. Kim, S.M. George, *J. Phys. Chem. C*, 114, 17597-17603, (2010).
13. T. H. Sajeesh, A. R. Warriar, C. Sudha Kartha, and K. P. Vijayakumar: *Thin Solid Films* 518, 4370, (2010).
14. S. Lopez and A. Ortiz: *Semicond. Sci. Technol.* 9, 2130, (1994).
15. A. Sanchez-Juarez and A. Ortiz: *J. Electrochem. Soc.* 147, 3708, (2000).
16. D. Patidar, N. Jain, N.S. Saxena, Kananbala Sharma, and T.P. Sharma: *Brazilian Journal of Physics.* 36, 1210, (2006).
17. Hebo, Zhongquanma, Xujing, Zhaolei, Zhangnansheng, Lifeng, Shencheng, Shenling, Mengxiajie, zhouchengyue, yuzhengshan, yinyanting: *Optica Applicata* 39(3), pp. 547–560, 2009.